Selective Disruption of the Cerebral Neocortex in Alzheimer's Disease

OPEN ACCESS Freely available online

PLoS one

Selective Disruption of the Cerebral Neocortex in Alzheimer's Disease

Rahul S. Desikan[1,2]*, Mert R. Sabuncu[1,12], Nicholas J. Schmansky[1], Martin Reuter[1], Howard J. Cabral[3], Christopher P. Hess[4], Michael W. Weiner[4,5], Alessandro Biffi[6,7], Christopher D. Anderson[6,7], Jonathan Rosand[6,7], David H. Salat[1], Thomas L. Kemper[8], Anders M. Dale[2,9], Reisa A. Sperling[1,10], Bruce Fischl[1,12], the Alzheimer's Disease Neuroimaging Initiative[¶]

1 Athinoula A. Martinos Center for Biomedical Imaging, Department of Radiology, Massachusetts General Hospital, Charlestown, Massachusetts, United States of America, **2** Department of Radiology, University of California San Diego, La Jolla, California, United States of America, **3** Department of Biostatistics, Boston University School of Public Health, Boston, Massachusetts, United States of America, **4** Department of Radiology, University of California San Francisco, San Francisco, California, United States of America, **5** Department of Veteran Affairs, San Francisco, California, United States of America, **6** Center for Human Genetic Research, Department of Neurology, Massachusetts General Hospital, Boston, Massachusetts, United States of America, **7** Program in Medical and Population Genetics, Broad Institute, Cambridge, Massachusetts, United States of America, **8** Department of Anatomy and Neurobiology, Boston University School of Medicine, Boston, Massachusetts, United States of America, **9** Department of Neuroscience, University of California San Diego, La Jolla, California, United States of America, **10** Center for Alzheimer Research and Treatment, Department of Neurology, Brigham and Women's Hospital, Boston, Massachusetts, United States of America, **11** Department of Neurology, Massachusetts General Hospital, Boston, Massachusetts, United States of America, **12** Computer Science and Artificial Intelligence Laboratory (CSAIL) and Harvard-MIT Division of Health Sciences and Technology, Massachusetts Institute of Technology, Cambridge, Massachusetts, United States of America

Abstract

Background: Alzheimer's disease (AD) and its transitional state mild cognitive impairment (MCI) are characterized by amyloid plaque and tau neurofibrillary tangle (NFT) deposition within the cerebral neocortex and neuronal loss within the hippocampal formation. However, the precise relationship between pathologic changes in neocortical regions and hippocampal atrophy is largely unknown.

Methodology/Principal Findings: In this study, combining structural MRI scans and automated image analysis tools with reduced cerebrospinal fluid (CSF) Aß levels, a surrogate for intra-cranial amyloid plaques and elevated CSF phosphorylated tau (p-tau) levels, a surrogate for neocortical NFTs, we examined the relationship between the presence of Alzheimer's pathology, gray matter thickness of select neocortical regions, and hippocampal volume in cognitively normal older participants and individuals with MCI and AD (n = 724). Amongst all 3 groups, only select heteromodal cortical regions significantly correlated with hippocampal volume. Amongst MCI and AD individuals, gray matter thickness of the entorhinal cortex and inferior temporal gyrus significantly predicted longitudinal hippocampal volume loss in both amyloid positive and p-tau positive individuals. Amongst cognitively normal older adults, thinning only within the medial portion of the orbital frontal cortex significantly differentiated amyloid positive from amyloid negative individuals whereas thinning only within the entorhinal cortex significantly discriminated p-tau positive from p-tau negative individuals.

Conclusions/Significance: Cortical Aβ and tau pathology affects gray matter thinning within select neocortical regions and potentially contributes to downstream hippocampal degeneration. Neocortical Alzheimer's pathology is evident even amongst older asymptomatic individuals suggesting the existence of a preclinical phase of dementia.

Citation: Desikan RS, Sabuncu MR, Schmansky NJ, Reuter M, Cabral HJ, et al. (2010) Selective Disruption of the Cerebral Neocortex in Alzheimer's Disease. PLoS ONE 5(9): e12853. doi:10.1371/journal.pone.0012853

Editor: Sérgio Teixeira Ferreira, Federal University of Rio de Janeiro, Brazil

Received May 14, 2010; **Accepted** August 28, 2010; **Published** September 23, 2010

Funding: The funders had no role in study design, data collection and analysis, decision to publish, or preparation of the manuscript. This work was supported by grants from the National Center for Research Resources (P41-RR14075, R01 RR 16594-01A1 and the NCRR BIRN Morphometric Project BIRN002, U24 RR021382), the National Institute for Biomedical Imaging and Bioengineering (R01 EB001550, R01EB006758), National Institute for Neurological Disorders and Stroke (R01 NS052585-01), the Mental Illness and Neuroscience Discovery (MIND) Institute, and the National Institute on Aging (P50 AG05681, P01 AG03991, AG02238 and AG021910). Additional support was provided by The Autism & Dyslexia Project funded by the Ellison Medical Foundation. Data collection and sharing for this project was funded by the Alzheimer's Disease Neuroimaging Initiative (ADNI) (National Institutes of Health Grant U01 AG024904). ADNI is funded by the National Institute on Aging, the National Institute of Biomedical Imaging and Bioengineering, and through generous contributions from the following: Abbott, AstraZeneca AB, Bayer Schering Pharma AG, Bristol-Myers Squibb, Eisai Global Clinical Development, Elan Corporation, Genentech, GE Healthcare, GlaxoSmithKline, Innogenetics, Johnson and Johnson, Eli Lilly and Co., Medpace, Inc., Merck and Co., Inc., Novartis AG, Pfizer Inc, F. Hoffman-La Roche, Schering-Plough, Synarc, Inc., as well as non-profit partners the Alzheimer's Association and Alzheimer's Drug Discovery Foundation, with participation from the U.S. Food and Drug Administration. Private sector contributions to ADNI are facilitated by the Foundation for the National Institutes of Health (www.fnih.org). The grantee organization is the Northern California Institute for Research and Education, and the study is coordinated by the Alzheimer's Disease Cooperative Study at the University of California San Diego. ADNI data are disseminated by the Laboratory for Neuro Imaging at the University of California Los Angeles. This research was also supported by NIH grants P30 AG010129, K01 AG030514, and the Dana Foundation.

Competing Interests: The authors have declared that no competing interests exist.

* E-mail: rahul@nmr.mgh.harvard.edu

¶ For more information on the Alzheimer's Disease Neuroimaging Initiative please see the Acknowledgments.

Introduction

Selective neurodegeneration of the cerebral cortex is a characteristic pathological feature of Alzheimer's disease (AD). Intracellular tau-associated neurofibrillary tangles (NFTs) and extracellular amyloid-ß (Aß) associated plaques show a characteristic laminar and regional pattern of distribution within gray matter, with greater involvement of the medial temporal lobe and heteromodal association areas than primary sensory or motor cortices [1–3]. Within heteromodal association cortices, long corticocortical projections and the large pyramidal neurons in layers III and V that give rise to these projections appear to be especially vulnerable [4,5]. As such, it has been postulated that early disruptions in heteromodal association cortices can contribute to a functional isolation of the hippocampal formation thus giving rise to the clinical hallmark of Alzheimer's disease, progressive memory impairment [6,7].

Recent advances in neuroimaging and image analysis algorithms allow for the *in vivo* assessment of neuropathologic changes underlying AD. Positron emission tomography (PET) studies examining fibrillar amyloid deposition with Pittsburgh Compound B (PiB) and MRI studies of functional and structural connectivity have observed a significant overlap in a number of neocortical regions that appear preferentially affected in the earliest stages of AD [8–14]. Taken collectively, these studies suggest that select heteromodal cortical regions are vulnerable to amyloid deposition and exhibit neuronal dysfunction early in the disease process. In comparison, though several studies have demonstrated a relationship between post-mortem NFT pathology and structural MRI measures of atrophy [15,16], few have examined *in vivo* the effect of tau burden on atrophy in heteromodal and limbic cortices.

Cortical atrophy resulting from cellular shrinkage, dendritic spine loss, and axonal disruption is reflected as a loss of gray matter that diminishes cortical thickness [17,18]. Prior MRI studies of AD have shown cortical thinning and gray matter disturbances in medial temporal [19–21], temporo-parietal [22–25], posterior cingulate and medial frontal cortices [10,26]. Still, the precise relationship between amyloid and tau pathology, regional neocortical thinning, and hippocampal atrophy is largely unknown. In this study, using significant reductions in cerebrospinal fluid (CSF) Aß levels as a surrogate for elevated intra-cranial amyloid plaques [27,28] and significant elevations in CSF phosphorylated tau levels as a surrogate for neocortical NFTs [29], we explored relationships between the presence of Alzheimer's pathology, thickness of select neocortical regions and the volume of the hippocampus.

Methods

Overview

All 724 participants were selected from the Alzheimer's disease Neuroimaging Initiative (ADNI) database (www.loni.ucla.edu/ADNI). The ADNI is a large multi-site collaborative effort launched in 2003 by the National Institute on Aging, the National Institute of Biomedical Imaging and Bioengineering, the Food and Drug Administration, private pharmaceutical companies and non-profit organizations as a public–private partnership aimed at testing whether serial MRI, PET, other biological markers and clinical and neuropsychological assessment can be combined to measure the progression of MCI and early AD. The Principal Investigator of this initiative is Michael Weiner, MD, and ADNI is the result of many co-investigators from a broad range of academic institutions and private corporations, with subjects recruited from over 50 sites across the US and Canada. For more information, please see http://www.adni-info.org.

Clinical Assessments and Group Characteristics

Each participant from the ADNI cohort was formally evaluated using eligibility criteria that are described in detail elsewhere (http://www.adni-info.org/index.php?option = com_content&task = view&id = 9&Itemid = 43). The institutional review boards of all participating institutions approved the procedures for this study. Written informed consent was obtained from all participants or surrogates. Briefly, experienced clinicians conducted independent semi-structured interviews with the participant and a knowledgeable collateral source that included a health history, neurological examination, the Mini-Mental State Examination [30], the CDR-Sum of Boxes [31], and a comprehensive neuropsychological battery.

As illustrated in Table 1, participants from the ADNI database were selected if they were clinically classified as:

- **CN** (n = 208) - Individuals who were cognitively normal at baseline and clinical follow-up (CDR 0).
- **MCI** (n = 353) – Individuals with mild cognitive impairment (MCI) defined using the revised MCI criteria [32].
- **AD** (n = 163) – Individuals who met criteria for probable AD [33] (CDR 1).

MRI image acquisition

All ADNI MRI scans were acquired at multiple sites using either a GE, Siemens, or Philips 1.5T system. Multiple high-resolution T1- weighted volumetric MP-RAGE scans were collected for each subject and the raw DICOM images were downloaded from the public ADNI site (http://www.loni.ucla.edu/ADNI/Data/index.shtml). Parameter values vary depending on scanning site and can be found at http://www.loni.ucla.edu/ADNI/Research/Cores/.

MRI Image Processing

All MRI scans were processed, with little to no manual intervention using the FreeSurfer software package (version 4.5), freely available at http://surfer.nmr.mgh.harvard.edu. A single MPRAGE MRI acquisition for each participant was normalized for intensity inhomogeneities to create an image volume with high contrast-to-noise [34]. The intensity-normalized volume was used to automatically locate the gray/white matter boundary

Table 1. Descriptive statistical information for the participants in the study (means listed with standard deviations in parentheses).

Diagnostic Group	CN	MCI	AD
Sample Size	208	353	163
Age	76.0 (4.9)	74.5 (7.4)	74.9 (7.5)
Percent Female	48%	37%	50%
Education	16.1 (2.8)	15.7 (3.0)	14.8 (3.2)
Mini Mental State Examination	29.1 (1.0)	27.0 (1.8)	23.3 (1.9)
CDR-Sum of Boxes	0	1.6 (0.9)	4.2 (1.6)
APOE-ε4 carrier status	27%	54%	66%
Mean Hippocampal Volume (head size corrected)	5.0 (0.54)	4.41 (0.66)	4.07 (0.66)

doi:10.1371/journal.pone.0012853.t001

(white matter surface) [35] and in turn, the gray/CSF boundary (gray matter surface) [36]. Cortical thickness measurements were then obtained by calculating the distance between these two boundaries across the entire cortical mantle of each hemisphere [36].

The neocortex of the brain on the MRI scans was then automatically subdivided into gyral-based regions of interest (ROIs). To accomplish this, a registration procedure was used that aligns the cortical folding patterns [37] and probabilistically assigns every point on the cortical surface to one of the 32 ROIs [38]. For the purposes of this study, we focused on 8 ROIs bilaterally corresponding to neocortical regions that prior neuropathological [1–3], neuroimaging [19–26], and amyloid [10,12] studies have demonstrated as being affected early in the course of AD. These regions included the 1) caudal portion of the middle frontal gyrus (includes inferior frontal sulcus), 2) medial portion of the orbital frontal cortex, 3) inferior parietal lobule (includes inferior parietal sulcus), 4) lateral portion of the occipital cortex, 5) inferior temporal gyrus, 6) entorhinal cortex, 7) temporal pole, and 8) isthmus portion of the cingulate cortex (includes posterior cingulate and retrosplenial cortices) (Figure 1). The hippocampus was automatically delineated based on an algorithm that uses a probabilistic atlas and examines variations in voxel intensities and spatial relationships to classify subcortical regions on MRI scans [39].

For longitudinal analysis, the baseline and one-year follow-up structural MRI scans were rigid body registered and an unbiased template volume was created [40]. All time points and the template images were then skull stripped, intensity normalized and segmented independently. The longitudinal segmentation results were then obtained by directly mapping the linear Talairach transform and the brain mask from the template to the baseline and follow-up timepoint, and by initializing other processing steps such as the non-linear warps and intensity normalizations with the results from the template. For the baseline and follow-up timepoint, a fused segmentation image that incorporates information of both time points was used as an initial estimate to guide the final delineation of the hippocampus. Atrophy rate of the hippocampus was defined as percent volume loss over the course of one year. A more detailed description of these procedures can be found in [40].

Cerebrospinal Fluid Measures

From the current ADNI sample, a number of individuals (n = 338) underwent lumbar puncture for CSF biomarker evaluation. Methods for CSF acquisition and biomarker measurement have been reported previously for this sample [28]. In brief, CSF was collected and stored at −80°C at the University of Pennsylvania ADNI Biomarker Core Laboratory. Amyloid beta from peptides 1–42 (Aβ) and tau phosphorylated at threonine 181 (p-tau) was measured using the multiplex xMAP Luminex platform (Luminex Corp, Austin TX) with Innogenetics (INNOBIA AlzBio3, Ghent, Belgium) immunoassay kit–based reagents. Using a previously established CSF-based Aβ cutoff value of 192 pg/ml and a p-tau cutoff value of 23 pg/ml [28], we classified MCI and AD individuals as 1) amyloid positive (n = 193, 43% female, mean age = 74.0, SD = 7.4), 2) amyloid negative (n = 48, 30% female, mean age = 75.9, SD = 8.0), 3) p-tau positive (n = 182, 44% female, mean age = 74.0, SD = 7.5), and 4) p-tau negative (n = 59, 30% female, mean age = 76.1, SD = 7.6). Similarly, we additionally classified CN individuals as a) amyloid positive (n = 35, 54% female, mean age = 76.3, SD = 5.1), b) amyloid negative (n = 61, 50% female, mean age = 75.6, SD = 5.3), c) p-tau positive (n = 34, 47% female, mean age = 77.8, SD = 5.9), and d) p-tau negative (n = 62, 30% female, mean age = 74.7, SD = 4.4). Of note, 46% (n = 16) of the amyloid positive individuals were additionally p-tau positive and 47% (n = 16) of the p-tau positive individuals were additionally amyloid positive.

Statistical Analysis

Spearman's rank correlation coefficients were first used to examine relationships between the mean thickness of the

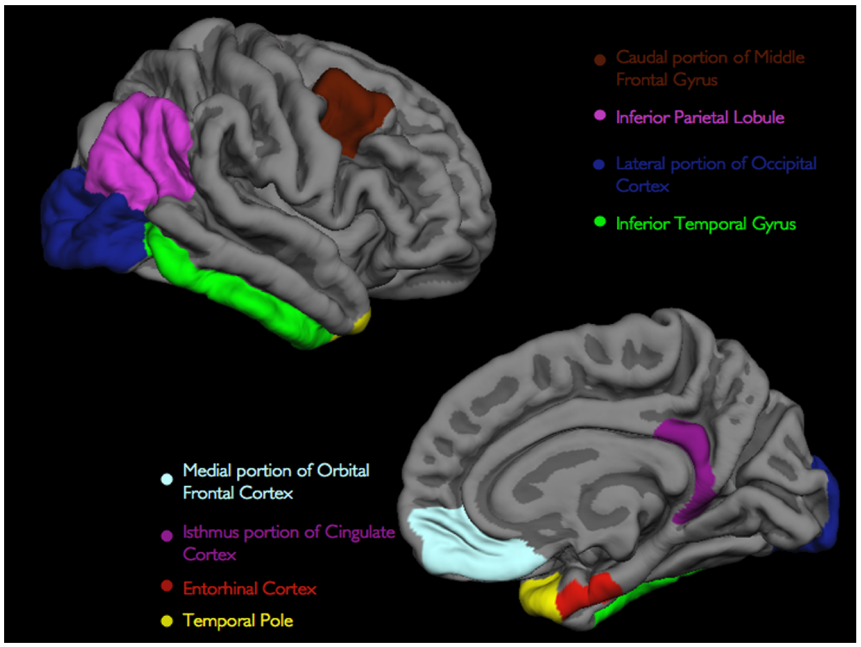

Figure 1. Three-dimensional representations of the 8 ROIs examined in the current study (only right hemisphere is shown). All of the ROIs visible in the lateral (top) and medial (bottom) views of the gray matter surface.
doi:10.1371/journal.pone.0012853.g001

Table 2. Correlation results between cortical thickness of eight neocortical ROIs and total hippocampal volume in all ADNI participants (n = 724).

Regions of Interest	HV	CMF	ERC	IPL	ITG	ISC	LOC	MOF	TP
HV	1	0.29	0.66	0.32	0.45	0.36	0.28	0.41	0.51
CMF		1	0.38	0.79	0.65	0.60	0.64	0.43	0.42
ERC			1	0.43	0.63	0.43	0.36	0.44	0.72
IPL				1	0.74	0.67	0.74	0.44	0.44
ITG					1	0.63	0.64	0.51	0.64
ISC						1	0.52	0.50	0.43
LOC							1	0.38	0.38
MOF								1	0.48
TP									1

Spearman's rank correlation coefficients listed, all p-values significant at <0.0001. All analyses included age, gender, education, and APOE-ε4 carrier status as co-variates. HV = Hippocampal volume, CMF = Caudal portion of middle frontal gyrus thickness, ERC = Entorhinal cortex thickness, IPL = Inferior parietal lobule thickness, ITG = Inferior temporal gyrus thickness, ISC = Isthmus portion of cingulate cortex thickness, LOC = Lateral portion of occipital cortex thickness, MOF = Medial portion of orbital frontal cortex thickness, TP = Temporal pole thickness.

doi:10.1371/journal.pone.0012853.t002

individual ROIs and total hippocampal volume. Separate linear regression models were constructed for the amyloid positive, amyloid negative, p-tau positive and p-tau negative MCI and AD individuals, with the baseline thickness of the individual ROIs as predictors for hippocampal atrophy rate. Logistic regression models and multivariate analysis of variance (MANOVA) were used to compare whether baseline thickness of the individual ROIs significantly differentiated amyloid positive from amyloid negative as well as p-tau positive from p-tau negative CN individuals. In all of the analyses performed, age, gender, education, and APOE-ε4 carrier status were additionally included.

Results

Correlations between regional neocortical thickness and hippocampal volume

Overall, the hippocampus demonstrated the largest magnitude of correlation with the entorhinal cortex (Spearman's $\rho = 0.66$, $p<0.001$), temporal pole (Spearman's $\rho = 0.51$, $p<0.001$), inferior temporal gyrus (Spearman's $\rho = 0.45$, $p<0.001$) and the medial portion of the orbital frontal cortex (Spearman's $\rho = 0.41$, $p<0.001$) (Table 2). The inferior parietal lobule and caudal portion of the middle frontal gyrus showed the strongest magnitude of correlation with each other and with the other neocortical regions (Table 2). Within the AD cohort, the hippocampus did not demonstrate any significant correlations with any of the lateral frontal, occipital, or parietal regions including the isthmus portion of the cingulate cortex (Spearman's $\rho = 0.12$, $p>0.05$) but correlated significantly with the entorhinal cortex (Spearman's $\rho = 0.57$, $p<0.001$), temporal pole (Spearman's $\rho = 0.38$, $p<0.001$), inferior temporal gyrus (Spearman's $\rho = 0.23$, $p<0.01$), and the medial portion of the orbital frontal cortex (Spearman's $\rho = 0.33$, $p<0.001$) (Table 3). In comparison, within MCI cohort, the hippocampus correlated significantly with each neocortical region (Table 4) and similarly, within the CN cohort the hippocampus correlated significantly with all neocortical regions except the lateral portion of the occipital cortex (Spearman's $\rho = 0.03$, $p>0.05$) (Table 5).

Regional cortical thickness, Aβ, and p-tau as predictors of hippocampal atrophy

Linear regression models amongst the MCI and AD individuals demonstrated that decreased Aβ levels (ß-coefficient = −0.08,

Table 3. Correlation results between cortical thickness of eight neocortical ROIs and total hippocampal volume in only AD individuals (n = 163).

Regions of Interest	HV	CMF	ERC	IPL	ITG	ISC	LOC	MOF	TP
HV	1	0.02 (NS)	0.57 (0.0001)	0.03 (NS)	0.23 (0.003)	0.12 (NS)	0.12 (NS)	0.33 (0.0001)	0.38 (0.0001)
CMF		1	0.17 (0.02)	0.77 (0.0001)	0.56 (0.0001)	0.58 (0.0001)	0.59 (0.0001)	0.27 (0.0005)	0.24 (0.002)
ERC			1	0.12 (NS)	0.49 (0.0001)	0.27 (0.007)	0.19 (0.01)	0.38 (0.0001)	0.67 (0.0001)
IPL				1	0.63 (0.0001)	0.64 (0.0001)	0.67 (0.0001)	0.24 (0.001)	0.23 (0.01)
ITG					1	0.58 (0.0001)	0.51 (0.0001)	0.46 (0.0001)	0.61 (0.0001)
ISC						1	0.49 (0.0001)	0.42 (0.0001)	0.34 (0.0001)
LOC							1	0.36 (0.0001)	0.29 (0.0001)
MOF								1	0.52 (0.0001)
TP									1

Spearman's rank correlation coefficients listed with p-values in parentheses. All analyses included age, gender, education, and APOE-ε4 carrier status as co-variates. HV = Hippocampal volume, CMF = Caudal portion of middle frontal gyrus thickness, ERC = Entorhinal cortex thickness, IPL = Inferior parietal lobule thickness, ITG = Inferior temporal gyrus thickness, ISC = Isthmus portion of cingulate cortex thickness, LOC = Lateral portion of occipital cortex thickness, MOF = Medial portion of orbital frontal cortex thickness, TPC = Temporal pole thickness, NS = Not significant.

doi:10.1371/journal.pone.0012853.t003

Table 4. Correlation results between cortical thickness of eight neocortical ROIs and total hippocampal volume in only MCI individuals (n = 353).

Regions of Interest	HV	CMF	ERC	IPL	ITG	ISC	LOC	MOF	TP
HV	1	0.18	0.61	0.21	0.36	0.28	0.27	0.32	0.48
CMF		1	0.27	0.76	0.63	0.57	0.59	0.43	0.34
ERC			1	0.31	0.55	0.31	0.30	0.37	0.73
IPL				1	0.72	0.65	0.71	0.40	0.37
ITG					1	0.58	0.61	0.47	0.59
ISC						1	0.48	0.48	0.37
LOC							1	0.33	0.31
MOF								1	0.43
TP									1

Spearman's rank correlation coefficients, all p-values significant at <0.0001. All analyses included age, gender, education, and APOE-ε4 carrier status as co-variates. HV = Hippocampal volume, CMF = Caudal portion of middle frontal gyrus thickness, ERC = Entorhinal cortex thickness, IPL = Inferior parietal lobule thickness, ITG = Inferior temporal gyrus thickness, ISC = Isthmus portion of cingulate cortex thickness, LOC = Lateral portion of occipital cortex thickness, MOF = Medial portion of orbital frontal cortex thickness, TPC = Temporal pole thickness.

doi:10.1371/journal.pone.0012853.t004

95% Confidence Interval (CI) = −0.01 to −0.003, $p<0.01$) and increased p-tau levels (ß-coefficient = 0.02, 95% CI = 0.006 to 0.03, $p<0.01$) significantly predicted hippocampal atrophy rate. Within the amyloid positive MCI and AD individuals, baseline thickness of the entorhinal cortex (ß-coefficient = −0.79, 95% CI = −1.20 to −0.37, $p<0.0001$) and inferior temporal gyrus (ß-coefficient = −1.04, 95% CI = −2.14 to −0.06, $p<0.05$) significantly predicted the atrophy rate of the hippocampus. Similarly, within the p-tau positive individuals, baseline thickness of the entorhinal cortex (ß-coefficient = −0.66, 95% CI = −1.09 to −0.23, $p<0.01$) and inferior temporal gyrus (ß-coefficient = −1.20, 95% CI = −2.31 to −0.10, $p<0.05$) significantly predicted the atrophy rate of the hippocampus (Figure 2). Within the amyloid negative and p-tau negative MCI and AD individuals, none of the neocortical regions significantly predicted longitudinal hippocampal atrophy.

Regional cortical thinning in cognitively normal older individuals

Logistic regression models amongst the CN cohort demonstrated that APOE-ε4 carrier status (Odds Ratio (OR) = 0.08, 95% CI = 0.02 to 0.27, $p<0.0001$) and thinning in the medial portion of the orbital frontal cortex (OR = 5.77, 95% CI = 1.12 to 44.80, $p<0.05$) significantly differentiated the amyloid positive from amyloid negative older individuals whereas thinning of the entorhinal cortex (OR = 2.99, 95% CI = 1.10 to 9.73, $p<0.05$) significantly differentiated the p-tau positive from p-tau negative older individuals (Figure 3). None of the other measures, including baseline hippocampal volume, showed any significant effects. A MANOVA confirmed that only APOE-ε4 carrier status ($F = 18.5$, $p<0.0001$) and thinning of the medial orbital frontal cortex significantly ($F = 3.73$, $p<0.05$) differentiated amyloid positive from amyloid negative individuals and only thinning of the entorhinal cortex ($F = 3.58$, $p<0.05$) significantly discriminated p-tau positive from p-tau negative individuals.

Discussion

Our results demonstrate that 1) amongst cognitively normal older participants and individuals with MCI and AD, select heteromodal association cortices correlate with hippocampal volume, 2) amongst MCI and AD individuals, gray matter thinning within the same two neocortical regions predicts

Table 5. Correlation results between cortical thickness of eight neocortical ROIs and total hippocampal volume in only CN individuals (n = 208).

Regions of Interest	HV	CMF	ERC	IPL	ITG	ISC	LOC	MOF	TP
HV	1	0.16 (0.02)	0.36 (0.0001)	0.15 (0.02)	0.20 (0.003)	0.19 (0.005)	0.03 (NS)	0.29 (0.0001)	0.23 (0.0005)
CMF		1	0.27 (0.0001)	0.76 (0.0001)	0.51 (0.0001)	0.49 (0.0001)	0.62 (0.0001)	0.34 (0.0005)	0.38 (0.002)
ERC			1	0.35 (0.0001)	0.52 (0.0001)	0.31 (0.007)	0.28 (0.0001)	0.37 (0.0001)	0.56 (0.0001)
IPL				1	0.63 (0.0001)	0.51 (0.0001)	0.75 (0.0001)	0.38 (0.001)	0.40 (0.01)
ITG					1	0.48 (0.0001)	0.57 (0.0001)	0.38 (0.0001)	0.49 (0.0001)
ISC						1	0.44 (0.0001)	0.38 (0.0001)	0.23 (0.0005)
LOC							1	0.31 (0.0001)	0.31 (0.0001)
MOF								1	0.35 (0.0001)
TP									1

Spearman's rank correlation coefficients listed with p-values in parentheses. All analyses included age, gender, education, and APOE-ε4 carrier status as co-variates. HV = Hippocampal volume, CMF = Caudal portion of middle frontal gyrus thickness, ERC = Entorhinal cortex thickness, IPL = Inferior parietal lobule thickness, ITG = Inferior temporal gyrus thickness, ISC = Isthmus portion of cingulate cortex thickness, LOC = Lateral portion of occipital cortex thickness, MOF = Medial portion of orbital frontal cortex thickness, TPC = Temporal pole thickness, NS = Not significant.

doi:10.1371/journal.pone.0012853.t005

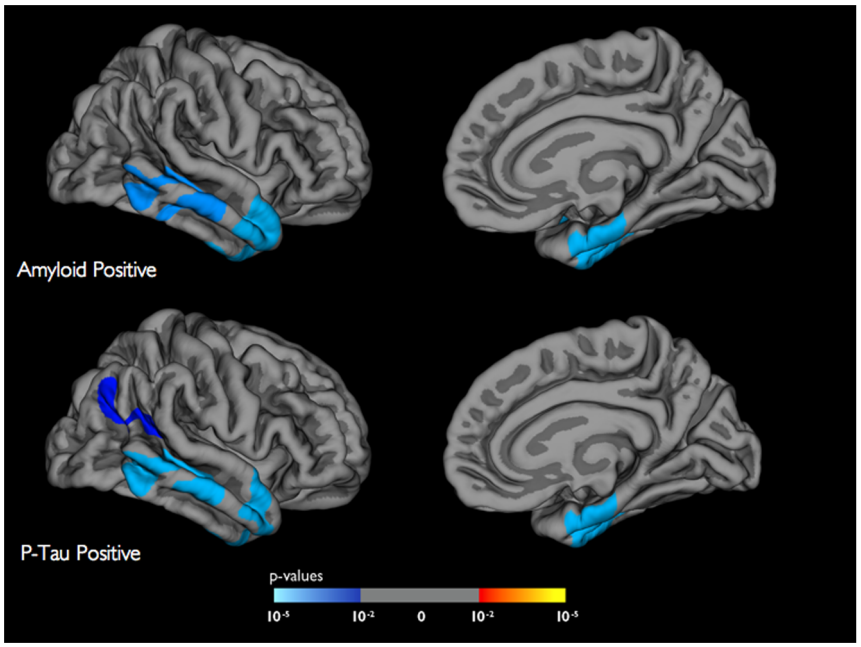

Figure 2. General linear model analyses demonstrating the prediction of longitudinal hippocampal atrophy (over one year) using baseline cortical thickness for the amyloid positive (top panel) and p-tau positive individuals (bottom panel). All results are corrected for multiple comparisons by method of Monte Carlo simulation and shown on the gray matter surface (only right hemisphere). The color scale illustrates the magnitude of effect with blue indicating areas of strongest prediction strength.
doi:10.1371/journal.pone.0012853.g002

longitudinal hippocampal volume loss in both amyloid positive and p-tau positive individuals and 3) amongst cognitively normal older adults, thinning within the medial portion of the orbital frontal cortex significantly differentiates amyloid positive from amyloid negative individuals whereas entorhinal cortex thinning significantly discriminates p-tau positive from p-tau negative individuals. Taken collectively, this indicates that cortical Aβ and tau pathology is evident even among asymptomatic older individuals, affects gray matter thinning within select neocortical regions and potentially contributes to downstream hippocampal degeneration. These findings are in agreement with prior work indicating the value of CSF Aβ as an early biomarker [41] and provide evidence that CSF p-tau and structural MRI measures are additionally informative in the earliest phase of the disease process.

Relationship between thickness of heteromodal regions and hippocampal volume

The four cerebral cortical regions that best correlated with hippocampal volume follow an interesting neurodevelopmental pattern. On architectonic grounds, the regions identified on the lateral hemisphere trace evolutionary lineage from the so-called 'paleocortical' trend whereas regions identified on the medial hemisphere are derived from the 'archicortical' trend [42–44]. As first described by Kemper [3], these regions collectively subserve the 'special senses of the head' including vision, memory, emotion, olfaction, and audition and are inherently heteromodal, binding convergent input from unimodal areas, thus acting as critical gateways for information processing and synthesis [45].

Correlations between thickness of the individual regions and hippocampal volume may reflect underlying patterns of neuropathology. Thickness of the medial portion of the orbital frontal cortex, inferior temporal gyrus, entorhinal cortex, and the temporal pole demonstrated the strongest magnitude of association with the hippocampus amongst each of the three participant groups. In contrast, parietal, occipital, and lateral frontal cortices, correlated with the hippocampus only amongst cognitively normal older adults and MCI individuals. With AD onset, these regions failed to associate with the hippocampus. Of interest, these regions showed the largest magnitude of association with each other amongst each of the three participant groups (Tables 3, 4 and 5).

One explanation for these findings may involve the evolution of the neuropathologic cascade in AD. Amyloid deposits are first noted in the medial portions of the orbital frontal, basal temporal and entorhinal cortices and tau-associated NFTs initially affect the medial temporal and temporopolar cortices [1,2]. With disease progression, these pathologic changes involve the parietal, primary occipital, and lateral frontal cortices [1–3]. Thus, those neocortical regions that show early pathologic changes may correlate with each other throughout the duration of the disease process whereas regions affected later may best associate with each other rather than earlier involved regions.

Another possibility is that associations between regions reflect underlying anatomic connections and the decreased correlation coefficients noted with AD onset represent a selective disruption in cortico-hippocampal connectivity. Though several studies have noted disruptions in anatomic connectivity with AD [8,13,46], the fact that the cognitively normal older adults when compared with the MCI and AD individuals demonstrated decreased correlation coefficients between several neocortical regions (including the entorhinal cortex) and the hippocampus (Table 5) suggests that the gray matter associations presented here likely do not represent cortico-hippocampal connectivity. Using diffusion tensor imaging with anatomic localization [47], future work will investigate whether cortico-hippocampal circuitry is selectively vulnerable in dementia.

Heteromodal cortices, Aβ, and p-tau as predictors of hippocampal atrophy

Significant reductions in CSF Aβ levels and elevations in CSF p-tau levels coupled with thinning within select heteromodal regions

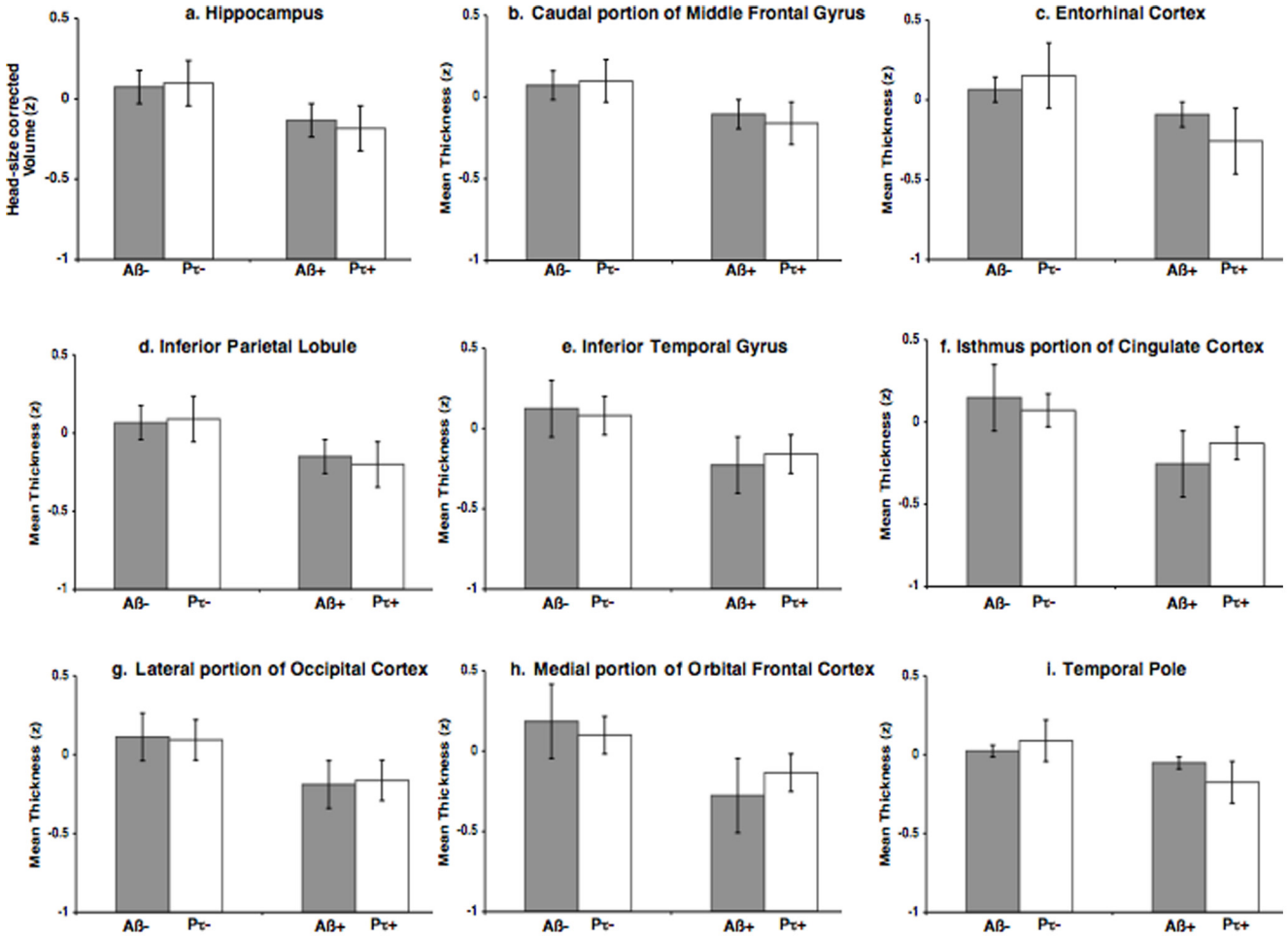

Figure 3. Bar plots illustrating mean cortical thickness, standardized to Z scores, for the 8 neocortical ROIs amongst the amyloid positive (Aβ+), amyloid negative (Aβ−), p-tau positive (Pτ+), and p-tau negative (Pτ−) older individuals. Error bars indicate 1 standard error of the mean.
doi:10.1371/journal.pone.0012853.g003

predicts longitudinal hippocampal atrophy. Prior PiB studies have demonstrated a significant relationship between neocortical amyloid deposition and hippocampal atrophy [48–51]. Our findings indicate that in addition to amyloid, tau may predict downstream hippocampal degeneration. Within both the amyloid and p-tau positive MCI and AD individuals, thickness of the same two neocortical regions (entorhinal cortex and inferior temporal gyrus) (Figure 2) significantly predicted hippocampal atrophy whereas within the amyloid and p-tau negative individuals none of the neocortical regions predicted hippocampal decline. This suggests that those neocortical regions that are likely affected by both Aβ and tau influence hippocampal degeneration.

Disruption of select heteromodal regions amongst asymptomatic older individuals – evidence for a 'preclinical' phase of dementia

Amongst cognitively normal older adults, cortical thinning of the medial orbital frontal cortex significantly differentiated amyloid positive from amyloid negative individuals whereas thinning of the entorhinal cortex significantly discriminated p-tau positive from p-tau negative individuals. Consistent with neuropathology studies, which demonstrate early amyloid deposition within the medial orbital frontal cortex and early NFT accumulation within the entorhinal cortex [1,2], our results indicate that Aβ and tau pathology differentially affect neocortical regions even among asymptomatic older individuals. To our knowledge, this is the first *in vivo* evidence that amongst cognitively normal individuals tau pathology selectively affects the thickness of the entorhinal cortex. It is important to note that almost half (47%) of the p-tau positive individuals were additionally amyloid positive and future work will involve looking at the interaction between Aβ and tau pathology.

The finding that amyloid positive individuals show selective thinning within the medial orbital frontal cortex is in agreement with one prior study demonstrating that older individuals with subjective memory complaints show significant correlations between gray matter atrophy and neocortical PiB increase within the medial orbital frontal/anterior cingulate cortex [52]. Additionally, this is compatible with functional connectivity studies illustrating that amyloid deposition amongst older individuals disrupts the 'default network', which includes the medial aspect of the prefrontal cortex [14,53]. Consistent with prior work [54,55], our results indicate that amongst asymptomatic older individuals APOE ε4 carrier status influences CSF Aβ levels but does not affect CSF p-tau levels. Taken together, this indicates that a number of cognitively normal individuals harbor preclinical

Alzheimer's pathology and that intracranial Aβ pathology may represent the biological phenotype of the APOE ε4 genotype.

Clinical Implications and Further Observations

These findings have important clinical implications. Subtle gray matter disturbances in specific regions of the cerebral neocortex are present amongst a subset of asymptomatic older individuals and can be quantified using sensitive structural neuroimaging techniques. In combination with CSF Aβ and tau, structural MRI measures can provide an indication of disease stage and have value in identifying those who will likely benefit from early therapeutic interventions. Our results also indicate the importance of administering anti-amyloid therapy early in the disease process (at a pre-MCI stage) in order to alter or delay hippocampal degeneration and thus progressive memory loss, the harbinger of clinical Alzheimer's dementia.

Why does neurodegeneration affect select cerebral cortical regions? From a phylogenetic perspective, heteromodal and archicortical medial temporal regions constitute the oldest areas of the brain [56], operating as connectional gateways for information synthesis [44,45], and as such, are likely subject to greater evolutionary selection pressure for degeneration than 'newer' brain regions such as the primary sensory areas. Another possibility is that those parts of the brain that need to sustain the highest level of plasticity are most susceptible to degeneration [57]. It is important to note that these two hypotheses need not be considered mutually exclusive. That is, the oldest and densely connected brain regions also presumably have the highest neuroplasticity demands and as such, may be particularly vulnerable to neuropathologic changes.

Limitations and Caveats

This study has several limitations. One issue involves the use of gyral-based neuroanatomic ROIs to examine specific neocortical regions. It is likely the case that Alzheimer's pathology does not follow the specific boundaries of these ROIs and affects areas within and across multiple ROIs. The use of regions of interest generated from a disease specific effect [19,20] presents one approach to overcome this limitation. However, as discussed in [58], this method can underestimate or miss disease specific effects potentially leading to false negative findings. Future work will involve combining *a priori* anatomically defined regions with disease-based statistical methods to examine neocortical and subcortical areas in AD. Another limitation involves the use of CSF Aβ and p-tau to assess the presence of amyloid and neurofibrillary pathology in the neocortex. Though amyloid load as measured using PiB and CSF Aβ are highly correlated and likely reflect plaque deposition [59], assessments using PiB may provide a more direct estimate of neocortical amyloid. Similarly, though prior work indicates that CSF p-tau and cortical NFTs are significantly correlated in AD [29], measurements using PET imaging agents that target tangle deposits [60] may offer a more exact estimate of neocortical neurofibrillary pathology.

Acknowledgments

Data used in the preparation of this article were obtained from the Alzheimer's Disease Neuroimaging Initiative (ADNI) database (www.loni.ucla.edu/ADNI). As such, the investigators within the ADNI contributed to the design and implementation of ADNI and/or provided data but ?did not participate in analysis or writing of this report. ADNI investigators include (complete listing available at www.loni.ucla.edu/ADNI/Collaboration/ADNI_Citation.shtml).

The authors would like to thank Craig Cloutier for his invaluable assistance with the development of the figures presented in this manuscript.

Author Contributions

Conceived and designed the experiments: RSD CPH MWW JR TLK AMD RAS BF. Performed the experiments: RSD MRS NJS HJC AB. Analyzed the data: RSD MRS NJS HJC AB CDA DHS. Contributed reagents/materials/analysis tools: MR BF. Wrote the paper: RSD MR CPH MWW AB CDA JR DHS TLK AMD RAS BF.

References

1. Arnold SE, Hyman BT, Flory J, Damasio AR, Van Hoesen GW (1991) The topographical and neuroanatomical distribution of neurofibrillary tangles and neuritic plaques in the cerebral cortex of patients with Alzheimer's disease. Cereb Cortex 1: 103–116.
2. Braak H, Braak E (1991) Neuropathological stageing of Alzheimer-related changes. Acta Neuropathol 82: 239–59.
3. Kemper TL (1994) in Clinical Neurology of Aging, Albert M, Knoefel J, eds. (Oxford University Press, New York). pp 3–78.
4. Morrison JH, Hof PR (1997) Life and death of neurons in the aging brain. Science 278: 412–419.
5. Hof PR, Morrison JH (2004) The aging brain: morphomolecular senescence of cortical circuits. Trends Neurosci 27: 607–613.
6. Hyman BT, Van Hoesen GW, Damasio AR, Barnes CL (1984) Alzheimer's disease: cell-specific pathology isolates the hippocampal formation. Science 225: 1168–1170.
7. Gomez-Isla T, Spires T, De Calignon A, Hyman BT (2008) Neuropathology of Alzheimer's disease. Handb Clin Neurol 89: 233–243.
8. Greicius MD, Srivastava G, Reiss AL, Menon V (2004) Default-mode network activity distinguishes Alzheimer's disease from healthy aging: evidence from functional MRI. Proc Natl Acad Sci U S A 101: 4637–4642.
9. Greicius MD, Supekar K, Menon V, Dougherty RF (2009) Resting-state functional connectivity reflects structural connectivity in the default mode network. Cereb Cortex 19: 72–78.
10. Buckner RL, Snyder AZ, Shannon BJ, LaRossa G, Sachs R, et al. (2005) Molecular, structural, and functional characterization of Alzheimer's disease: evidence for a relationship between default activity, amyloid, and memory. J Neurosci 25: 7709–7717.
11. Buckner RL, Andrews-Hanna JR, Schacter DL (2008) The brain's default network: anatomy, function, and relevance to disease. Ann N Y Acad Sci 1124: 1–38.
12. Buckner RL, Sepulcre J, Talukdar T, Krienen FM, Liu H, et al. (2009) Cortical hubs revealed by intrinsic functional connectivity: mapping, assessment of stability, and relation to Alzheimer's disease. J Neurosci 29: 1860–1873.
13. Seeley WW, Crawford RK, Zhou J, Miller BL, Greicius MD (2009) Neurodegenerative diseases target large-scale human brain networks. Neuron 62: 42–52.
14. Sperling RA, Laviolette PS, O'Keefe K, O'Brien J, Rentz DM, et al. (2009) Amyloid deposition is associated with impaired default network function in older persons without dementia. Neuron 63: 178–188.
15. Vemuri P, Whitwell JL, Kantarci K, Josephs KA, Parisi JE, et al. (2008) Antemortem MRI based STructural Abnormality iNDex (STAND)-scores correlate with postmortem Braak neurofibrillary tangle stage. Neuroimage 42: 559–67.
16. Whitwell JL, Josephs KA, Murray ME, Kantarci K, Przybelski SA, et al. (2008) MRI correlates of neurofibrillary tangle pathology at autopsy: a voxel-based morphometry study. Neurology 71: 743–9.
17. Narr KL, Toga AW, Szeszko P, Thompson PM, Woods RP, et al. (2005) Cortical thinning in cingulate and occipital cortices in first episode schizophrenia. Biol Psychiatry 58: 32–40.
18. Shaw P, Kabani NJ, Lerch JP, Eckstrand K, Lenroot R, et al. (2008) Neurodevelopmental trajectories of the human cerebral cortex. J Neurosci 28: 3586–3594.
19. Dickerson BC, Bakkour A, Salat DH, Feczko E, Pacheco J, et al. (2009) The cortical signature of Alzheimer's disease: regionally specific cortical thinning relates to symptom severity in very mild to mild AD dementia and is detectable in asymptomatic amyloid-positive individuals. Cereb Cortex 19: 497–510.
20. Bakkour A, Morris JC, Dickerson BC (2009) The cortical signature of prodromal AD: regional thinning predicts mild AD dementia. Neurology 72: 1048–1055.
21. Desikan RS, Cabral HJ, Hess CP, Dillon WP, Glastonbury CM, et al. (2009) Automated MRI measures identify individuals with mild cognitive impairment and Alzheimer's disease. Brain 132: 2048–2057.
22. Thompson PM, Mega MS, Woods RP, Zoumalan CI, Lindshield CJ, et al. (2001) Cortical change in Alzheimer's disease detected with a disease-specific population-based brain atlas. Cereb Cortex 11: 1–16.
23. Thompson PM, Hayashi KM, de Zubicaray G, Janke AL, Rose SE, et al. (2003) Dynamics of gray matter loss in Alzheimer's disease. J Neurosci 23: 994–1005.

24. Whitwell JL, Przybelski SA, Weigand SD, Knopman DS, Boeve BF, et al. (2007) 3D maps from multiple MRI illustrate changing atrophy patterns as subjects progress from mild cognitive impairment to Alzheimer's disease. Brain 130: 1777–1786.
25. Desikan RS, Fischl B, Cabral HJ, Kemper TL, Guttmann CR, et al. (2008) MRI measures of temporoparietal regions show differential rates of atrophy during prodromal AD. Neurology 71: 819–825.
26. Scahill RI, Schott JM, Stevens JM, Rossor MN, Fox NC (2002) Mapping the evolution of regional atrophy in Alzheimer's disease: unbiased analysis of fluid-registered serial MRI. Proc Natl Acad Sci U S A 99: 4703–4707.
27. DeMattos RB, Bales KR, Parsadanian M, O'Dell MA, Foss EM, et al. (2002) Plaque-associated disruption of CSF and plasma amyloid-beta (Abeta) equilibrium in a mouse model of Alzheimer's disease. J Neurochem 81: 229–236.
28. Shaw LM, Vanderstichele H, Knapik-Czajka M, Clark CM, Aisen PS, et al. (2009) Cerebrospinal fluid biomarker signature in Alzheimer's disease neuroimaging initiative subjects. Ann Neurol 65: 403–413.
29. Buerger K, Ewers M, Pirttilä T, Zinkowski R, Alafuzoff I, et al. (2006) Brain 129: 3035–41.
30. Folstein M, Folstein S, McHugh P (1975) "Mini-Mental State". A practical method for grading the cognitive state of patients for the clinician. J Psychiatr Res 12: 189–198.
31. Morris JC (1993) The Clinical Dementia Rating (CDR): current version and scoring rules. Neurology 43: 2412–2414.
32. Petersen RC (2004) Mild cognitive impairment as a diagnostic entity. J Intern Med 3: 183–94.
33. McKhann G, Drachman D, Folstein MF, Katzman R, Price D, et al. (1984) Clinical diagnosis of Alzheimer's disease: Report of the NINCDS-ADRDA Work group under the auspices of Department of Health and Human Services Task Force. Neurology 34: 939–944.
34. Dale AM, Fischl B, Sereno MI (1999) Cortical surface-based analysis. I. Segmentation and surface reconstruction. Neuroimage 9: 179–194.
35. Fischl B, Sereno MI, Dale AM (1999) Cortical surface-based analysis. II: Inflation, flattening, and a surface-based coordinate system. Neuroimage 9: 195–207.
36. Fischl B, Dale AM (2000) Measuring the thickness of the human cerebral cortex from magnetic resonance images. Proc Natl Acad Sci USA 97: 11050–11055.
37. Fischl B, Sereno MI, Tootell RB, Dale AM (1999) High-resolution intersubject averaging and a coordinate system for the cortical surface. Hum Brain Map 8: 272–284.
38. Desikan RS, Ségonne F, Fischl B, Quinn BT, Dickerson BC, et al. (2006) An automated labeling system for subdividing the human cerebral cortex on MRI scans into gyral based regions of interest. Neuroimage 31: 968–80.
39. Fischl B, Salat DH, Busa E, Albert M, Dieterich M, et al. (2002) Whole brain segmentation: automated labeling of neuroanatomical structures in the human brain. Neuron 33: 341–355.
40. Reuter M, Rosas HD, Fischl B (2010) Highly Accurate Inverse Consistent Registration: A Robust Approach. Neuroimage, Jul 13.
41. Jack CR, Jr., Knopman DS, Jagust WJ, Shaw LM, Aisen PS, et al. (2010) Hypothetical model of dynamic biomarkers of the Alzheimer's pathological cascade. Lancet Neurol 9: 119–128.
42. Sanides F (1969) Comparative architectonics of the neocortex of mammals and their evolutionary interpretation. Ann NY Acad Sci 167: 404–423.
43. Pandya DN, Yeterian EH (1985) in Cerebral Cortex, volume 4, Peters A, Jones EG, eds. (Plenum Press, New York). pp 3–55.
44. Pandya DN, Yeterian EH (1990) Neurobiology of higher cognitive function, Scheibel AB, Weschler AF, eds. (Guilford Press, New York). pp 53–84.
45. Mesulam MM (1998) From sensation to cognition. Brain 121: 1013–1052.
46. He Y, Chen Z, Evans A (2008) Structural insights into aberrant topological patterns of large-scale cortical networks in Alzheimer's disease. J Neurosci 28: 4756–4766.
47. Hagmann P, Cammoun L, Gigandet X, Meuli R, Honey CJ, et al. (2008) Mapping the structural core of human cerebral cortex. PLoS Biol 6: e159.
48. Mormino EC, Kluth JT, Madison CM, Rabinovici GD, Baker SL, et al. (2009) Episodic memory loss is related to hippocampal-mediated beta-amyloid deposition in elderly subjects. Brain 132: 1310–23.
49. Jack CR, Jr., Lowe VJ, Senjem ML, Weigand SD, Kemp BJ, et al. (2008) 11C PiB and structural MRI provide complementary information in imaging of Alzheimer's disease and amnestic mild cognitive impairment. Brain 131: 665–80.
50. Bourgeat P, Chételat G, Villemagne VL, Fripp J, Raniga P, et al. (2010) Beta-amyloid burden in the temporal neocortex is related to hippocampal atrophy in elderly subjects without dementia. Neurology 74: 121–7.
51. Frisoni GB, Lorenzi M, Caroli A, Kemppainen N, Någren K, et al. (2009) In vivo mapping of amyloid toxicity in Alzheimer disease. Neurology 72: 1504–11.
52. Chételat G, Villemagne VL, Bourgeat P, Pike KE, Jones G, et al. (2010) Relationship between atrophy and beta-amyloid deposition in Alzheimer disease. Ann Neurol 67: 317–24.
53. Hedden T, Van Dijk KR, Becker JA, Mehta A, Sperling RA, et al. (2009) Disruption of functional connectivity in clinically normal older adults harboring amyloid burden. J Neurosci 29: 12686–94.
54. Vemuri P, Wiste HJ, Weigand SD, Knopman DS, Shaw LM, et al. (2010) Effect of apolipoprotein E on biomarkers of amyloid load and neuronal pathology in Alzheimer disease. Ann Neurol 67: 308–16.
55. Morris JC, Roe CM, Xiong C, Fagan AM, Goate AM, et al. (2010) APOE predicts amyloid-beta but not tau Alzheimer pathology in cognitively normal aging. Ann Neurol 67: 122–31.
56. Yakovlev PI (1948) Motility, behavior, and the brain. J Nerv Ment Dis 107: 313–335.
57. Mesulam MM (1999) Neuroplasticity failure in Alzheimer's disease: bridging the gap between plaques and tangles. Neuron 24: 521–529.
58. Wolk DA, Dickerson BC (2010) Apolipoprotein E (APOE) genotype has dissociable effects on memory and attentional-executive network function in Alzheimer's disease. Proc Natl Acad Sci U S A 107: 10256–61.
59. Fagan AM, Mintun MA, Mach RH, Lee SY, Dence CS, et al. (2006) Inverse relation between in vivo amyloid imaging load and cerebrospinal fluid Abeta42 in humans. Ann Neurol 59: 512–519.
60. Small GW, Kepe V, Ercoli LM, Siddarth P, Bookheimer SY, et al. (2006) PET of brain amyloid and tau in mild cognitive impairment. N Engl J Med 355: 2652–63.